Hydrogen Generation with MoS_2

DOI: 10.1002/ange.201306918

Highly Effective Visible-Light-Induced H_2 Generation by Single-Layer 1T-MoS_2 and a Nanocomposite of Few-Layer 2H-MoS_2 with Heavily Nitrogenated Graphene

*Urmimala Maitra, Uttam Gupta, Mrinmoy De, Ranjan Datta, A. Govindaraj, and C. N. R. Rao**

Over the past decade, replacing fossil fuels by renewable sources of energy has become a major research goal not only because of the dwindling resources of fossil fuels but also due to harmful effects of CO_2 and other gases produced by combustion of the fuels. Hydrogen produced from water using solar energy is clearly the ultimate source of clean renewable energy. Traditionally, H_2 is generated from water using Pt electrodes, and several catalysts have been used for electrocatalytic, photocatalytic or photoelectrocatalytic production of hydrogen.[1] MoS_2, which is an established catalyst for the hydrodesulfurization reaction[2] has proven to be a good catalyst for electrochemical as well as photochemical hydrogen evolution reaction (HER).[3] Theoretical and experimental studies indicate that edges of MoS_2 are catalytically active while the basal plane remains inert.[4] Nanoparticles of MoS_2 with single-layered truncated triangular morphology with exposed Mo edges,[4b,5] or those grown on highly ordered pyrolytic graphite[6] or graphitic carbon[7] are catalytically active. Electrochemical HER carried out with nanoparticles of MoS_2 supported on carbon[8] and fluorine-doped tin oxide electrode[9] show higher yields of H_2. Hydrogen evolution appears to be further enhanced by using graphene[10] or carbon nanotubes[3a] to support nanocrystalline MoS_2, the favorable conductivity of the nanocarbons ensuring efficient electron transfer to the electrodes. Good photo-electrocatalytic activity of MoS_2 has been reported, with MoS_2 possessing the double gyroid structure with a large number of interconnected pores showing the highest efficiency.[11]

While electrochemical HER by MoS_2 has been studied in detail, photocatalytic HER by MoS_2 has received less attention. Bulk MoS_2 being an indirect band gap (1.29 eV) semiconductor does not absorb the solar spectrum efficiently. On sensitization with $[Ru(bpy)_3]^{2+}$ ions colloidal MoS_2 nanoparticles show photocatalytic HER activity with a turn over number (TON) of 93. The method utilizes a three-component system with ascorbic acid as the reductive quencher for excited state $[Ru(bpy)_3]^{2+}$ which in turn transfers electrons to MoS_2.[12] MoS_2 loaded on TiO_2[13] and CdS[14] has been investigated for H_2 evolution where TiO_2 and CdS act as both light absorbers and catalysts. Few-layer MoS_2 loaded on reduced graphene oxide (RGO) shows good HER activity compared to MoS_2 or its physical mixture with RGO, with EosinY as sensitizer.[15] Because graphene acts as a channel for transferring electrons to MoS_2 in graphene–MoS_2 composites we have carried out investigations on visible-light driven H_2 generation by few-layer 2H-MoS_2 (2H-MoS_2 and 1T-MoS_2 are polytypes of MoS_2, see Figure3c for structural models) and its composites with nitrogen-doped graphene. Nitrogen incorporation in graphene is expected to improve the catalytic activity of the composite with 2H-MoS_2 layers since it enhances the electron donating ability of the graphene. We have been able to prepare a MoS_2 composite with heavily nitrogenated RGO (% N ca. 15) which shows excellent HER activity. On analogous principles[16] it was demonstrated that the enhancement in electrocatalytic activity is due to the formation of a p–n junction in composites of n-type N-doped graphene with p-type MoS_2. Note that though the overall reaction is the photocatalytic generation of H_2, the electrons involved in the reduction of H_2O are not photocatalytically generated on MoS_2, but transferred from photogenerated species EY^- (EY = Eosin) to MoS_2.[15] It occurred to us that it would be more rewarding if the MoS_2 layer itself can be made more conducting. With this in mind, we have prepared MoS_2 by Li intercalation followed by exfoliation which yielded single-layers in the 1T form which is metallic. Our studies with 1T-MoS_2 have shown extraordinary results in H_2 evolution with a high turn-over frequency (TOF) of 6.25 h^{-1}.

In Figure 1 we show the yield of H_2 evolved on using the graphene (EG)-MoS_2(2H) composite with exfoliated graphene (EG) prepared by the thermal exfoliation of graphite oxide (XRD, TEM in Figure S1 and S2 of the Supporting Information). The composite exhibits much better H_2 evolution (0.54 mmol g^{-1} h^{-1}) than 2H-MoS_2 alone (0.05 mmol g^{-1} h^{-1}). After 4 h, the evolution, is 0.18 mmol g^{-1} with MoS_2 alone compared to approximately 1.8 mmol g^{-1} with EG-MoS_2 composite (atom % of Mo = 3 %). The presence of graphene prolongs the lifetime of the singly excited EY which then produces low-lying triplet excited state of EY (EY^{3*}), followed by the formation of EY^-. Graphene thus acts as an electron collector and transports the photogenerated electrons from highly reductive species EY^-[15] to catalytically active sites of 2H-MoS_2. The rate of H_2 evolution increased significantly to 0.83 mmol g^{-1} h^{-1} for MoS_2 composite with N-doped (% N = 5) EG (NEG) as shown in Figure 1. This is because 2H-MoS_2 being a p-type semiconductor accepts electrons from N-doped graphene. Thus, NEG-MoS_2(2H) (atom % of Mo = 3, XPS in Figure S3) shows a TOF of 0.45 h^{-1} which it is 2.1 times higher than that with

[*] U. Maitra, U. Gupta, Dr. M. De, Dr. R. Datta, Dr. A. Govindaraj, Prof. Dr. C. N. R. Rao
Chemistry and Physics of Materials Unit, International Centre for Materials Science, Sheik Saqr Laboratory and CSIR Centre of Excellence in Chemistry, Jawaharlal Nehru Centre for Advanced Scientific Research
Jakkur P. O., Bangalore 560 064 (India)
E-mail: cnrrao@jncasr.ac.in

Supporting information for this article is available on the WWW under http://dx.doi.org/10.1002/anie.201306918.

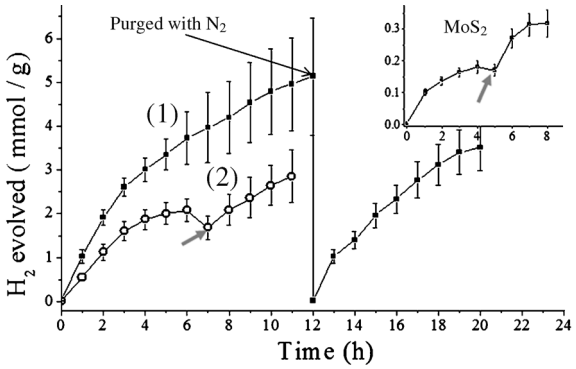

Figure 1. a) H_2 evolved per gram of catalyst by composites of few-layer 2H-MoS_2 with 1) NEG and 2) EG. Inset: time course of H_2 evolved by few-layer 2H-MoS_2. Arrow indicates addition of EY. The rate of H_2 evolution remains constant after purging.

EG-MoS_2(2H) and 57 times higher than with 2H-MoS_2 alone. Accordingly, the Raman G band (the G band is the in-plane stretching mode of graphene) of NEG shows large blue-shift of 11 cm^{-1} in the composite as a result of electron transfer to MoS_2 (see Figure S4 and Table ST1).[17] The trend in H_2 evolution was NEG-MoS_2 > EG-MoS_2 > MoS_2 independent of whether the few-layer MoS_2 was prepared by the solid-state reaction using thiourea or by the hydrothermal reaction[18] (see Figure S5).

Since our studies showed the yield of H_2 production to depend on the degree of N-doping in graphene as well as the MoS_2 content, we prepared composites of few-layer-2H-MoS_2 with heavily nitrogenated RGO, designated NRGO, (15% N, XPS in Figure S6), by an in situ procedure (see Experimental Section). Raman studies showed large stiffening of the G band of NRGO in the composite (Figure S4 and Table ST1). Clearly, there is strong electronic coupling between N-doped graphene and MoS_2, with the N-doped graphene donating electrons to MoS_2. Figure 2 shows the time course of H_2 evolved by NRGO-MoS_2 (atom% of Mo = 22) in comparison with that of RGO-MoS_2 (atom% of Mo = 24). We observe an initial H_2 evolution of 10.8 mmol g^{-1} h^{-1} H_2, with a high TOF of 2.9 h^{-1}. The yield of H_2 is nearly 3.5 times higher than that found with RGO-MoS_2 (3 mmol g^{-1} h^{-1} as shown in Figure 2) and about 200 times higher that MoS_2 alone. N-doping makes graphene electron-rich. MoS_2 being p-type, accepts electrons more readily from the electron-rich NRGO than from RGO. These results are consistent with the electrochemical measurements on composite electrodes such as N-doped RGO/MoS_2 and C_3N_4/N-doped graphene/MoS_2.[16] The morphology of MoS_2 on the graphene surface could also play a role in producing such high TOF. It is documented that only the edge sites of 2H-MoS_2 are catalytically active.[4a,19] TEM images of composites (Figure S7) show curling of the sheets to expose the catalytically active edges. Charge transfer to the edges is better when MoS_2 has grown vertically on graphene. Table 1 shows a comparison of photocatalytic yields and TOF values of various MoS_2-based catalysts. For proper comparison with earlier reported values, experiments were carried out with a 400 W Xe lamp as well. Under such conditions, the NRGO-MoS_2 nanocomposite gave an yield of 42 mmol g^{-1} h^{-1} which is about 940 mL g^{-1} h^{-1}, the TOF value being 11.5 h^{-1} which is highest value reported to date. The catalyst retains similar activity even after 6 cycles of 6 h each, with 0.075 mmol of the dye being replenished every 12 h (Figure S8).

Table 1: Activity of catalyst in terms of yield of H_2 evolved and TON.

Photocatalyst	Light source	Activity [mmol g^{-1} h^{-1}]	TOF[a] [h^{-1}]
Colloidal MoS_2[c][12]	300 W Xe lamp	–	6
MoS_2/CdS[14]	300 W Xe lamp	5.3	ca. 0.7
CdSe-MoS_2[32]	300 W Xe lamp	0.8	ca. 0.15
MoS_2/SiO_2[33]	Hg Lamp	0.86	ca. 0.14
MoS_2/TiO_2[34]	300 W Xe lamp	0.03	ca. 0.005
TiO_2/MoS_2/graphene[35]	300 W Xe lamp	2.1	ca. 0.35
MoS_xC_y[36]	300W Xe lamp	19	ca. 3
RGO-MoS_2[15]	300 W Xe lamp	2	–
MoS_2	100 W halogen	0.05,[b] 0.05	0.008,[b] 0.008
EG-MoS_2	100 W halogen	0.54,[b] 0.21	0.21,[b] 0.06
NEG-MoS_2	100 W halogen	0.83,[b] 0.54	0.45,[b] 0.144
RGO-MoS_2	100 W halogen	3	0.68
NRGO-MoS_2	100 W halogen	10.8	2.9
	400 W halogen	42	11.5
1T MoS_2	100 W halogen	26	6.2

[a] TOF calculated per mole of catalytically active material (Graphene and SiO_2 considered as catalytically inactive). [b] For samples prepared by solid-state method. [c] Sensitized with $[Ru(bpy)_3]^{2+}$ ions.

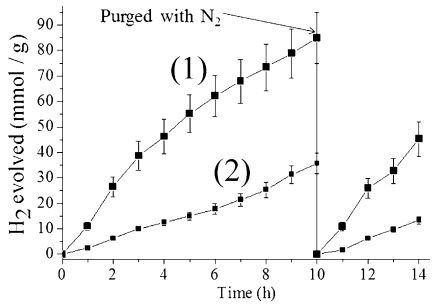

Figure 2. Time course of H_2 evolved by 1) NRGO-MoS_2 and 2) RGO-MoS_2 per gram of catalyst. After 10 h of H_2 evolution, the vessel was purged. The rate of H_2 evolution remains constant after purging.

Since graphene plays a vital role as an electron transporter to MoS_2 it seemed to us that increasing the conductivity of MoS_2 itself would favor HER. There is some evidence for a direct relation between catalytic activity and metallic character of MoS_2 edges.[5,6,20] While few-layer 2H-MoS_2 is semiconducting with an indirect band gap of 1.2 eV, the 1T polytype of MoS_2 is metallic.[21] We expected 1T-MoS_2 to be more efficient as a H_2 evolution catalyst by virtue of its metallic conductivity. Single-layer 1T-MoS_2 was prepared by Li-intercalation of bulk MoS_2 and subsequent exfoliation in water.[22] The electron diffraction pattern and the HRTEM images of 2H and 1T MoS_2 are given in Figure 3. The electron diffraction pattern of 2H-MoS_2 shows the usual hexagonal spot pattern (Figure 3a), but 1T-MoS_2 shows an extra

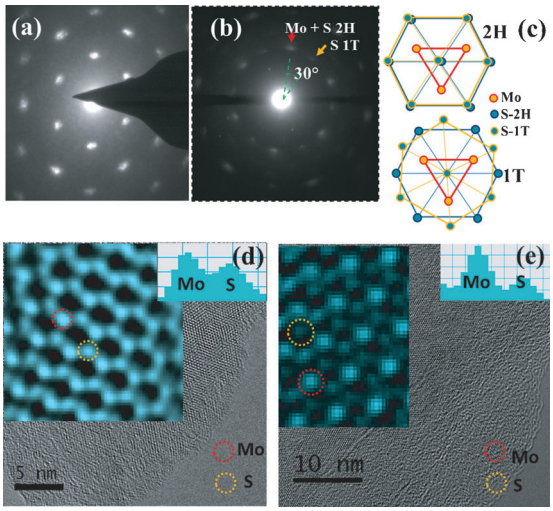

Figure 3. Electron diffraction patterns from single-layer MoS_2 with a) the 2H and b) 1T structures. c) Schematic structural model corresponding to the 2H and 1T structures. HRTEM images of the d) 2H and e) 1T structures. The insets in (d) and (e) show magnified images of Mo and S atomic arrangements in 2H and 1T structures as well as intensity line scans through Mo and S atoms.

hexagonal spot at 30° angular spacing in between the hexagonal spots of the 2H structure (Figure 3b). Figure 3c shows the schematic representation of 2H- and 1T-MoS_2 structures. 2H-MoS_2 has trigonal prismatic arrangement of Mo and S atoms, with the S atoms in the lower layer lying directly below those of the upper layer. In 1T-MoS_2, on the other hand, the S atoms in the upper and lower planes are offset from each other by 30° such that the Mo atoms lie in the octahedral holes of the S layers. The extra spot in electron diffraction arises from this rotation of one of the S atomic layers with respect to another. Figure 3d and 3e show the HRTEM images for single layer of 2H-MoS_2 and 1T-MoS_2. In case of 2H-MoS_2 three S atoms surrounds one Mo atom whereas for the 1T structure six S atoms can be seen surrounding one Mo atom. Intensity line scans through Mo and S atoms show a higher intensity difference for the 1T structure (one S atom in projection) compared to the 2H structure (2 S atoms together in projection). This difference in contrast is related to the corresponding phase shift (related to the net atomic number) under negative C_s (third-order spherical aberration coefficient) imaging conditions.[23]

The time course of H_2 evolution of single-layer 1T-MoS_2 is shown in Figure 4. This catalyst evolved almost 30 mmol $g^{-1}h^{-1}$ of H_2, 600 times higher than few-layer 2H-MoS_2 (Figure 1). Even under 100 W irradiation, the TOF of the catalyst is estimated to be 6.2 h^{-1}, higher than any MoS_2-based system reported to date. The highest TOF reported thus far is 6 h^{-1} for $[Ru(bpy)_3]^{2+}$-sensitized colloidal MoS_2 nanoparticles under 300 W Xe lamp (see Table 1). 1T-MoS_2 evolves around 250 mmol of H_2 corresponding to about 5.6 L of H_2 per gram of MoS_2 for 10 h. No significant quenching of the dye was observed even after 30 h of reaction indicating that photogenerated EY^- transfers electrons to 1T-MoS_2 efficiently (Figure S9). 1T-MoS_2 is reported to get converted into the 2H-MoS_2 analogue on annealing under

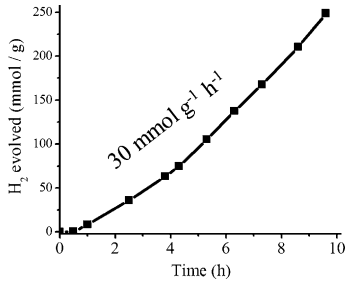

Figure 4. Time course of H_2 evolved by freshly prepared 1T-MoS_2.

inert atmosphere.[22] On drying the 1T-MoS_2 dispersion, the catalytic activity reduces only slightly from 30 mmol $g^{-1}h^{-1}$ to 24 mmol $g^{-1}h^{-1}$ but, there is a drastic reduction in the catalytic activity of the annealed sample, with rate of H_2 evolved being only 2.5 mmol $g^{-1}h^{-1}$ a value closer to that found with 2H-MoS_2 (Figure S10). The 1T phase, of MoS_2 being the metastable polytype of MoS_2, readily undergoes transition to more stable 2H polytype with time.[22] We therefore carried out photocatalytic H_2 evolution studies on fresh and 1 month old samples. The rate of H_2 evolution reduced only slightly over this period from 30 mmol $g^{-1}h^{-1}$ to 26 mmol $g^{-1}h^{-1}$ (Figure S11). These results are in accordance with electrochemical measurements of Lukowski et al.[24] and Voiry et al.[25] for metallic 1T polytypes of MoS_2 and WS_2. Preliminary measurements suggest 1T-$MoSe_2$ shows HER activity similar to 1T-MoS_2.

As illustrated by Tenne et al.,[21d] in the case of 2H-MoS_2, the valence band (VB) is composed of s3p states which is below the Fermi level by approximately 3.5 eV. The conduction band (CB) composed of Mo 4d states that lie just above the Fermi level leading to a narrow band gap. In terms of crystal-field theory, it can be described as hexagonal (D_{3h}) symmetry-induced splitting Mo 4d orbitals into three orbitals of closely spaced energies: one $4d_{z^2}$ and four doubly degenerate orbitals composed of$4d_{xy,x^2-y^2}$ and $4d_{xz,yz}$ as shown in Figure 5. Mo $4d_{z^2}$ is occupied and spin paired forming the VB, while the other four orbitals form the empty CB. As in 2H-MoS_2, VB of 1T-MoS_2 is composed of s3p which lie 3 eV below the Fermi level while the Mo 4d hosts the

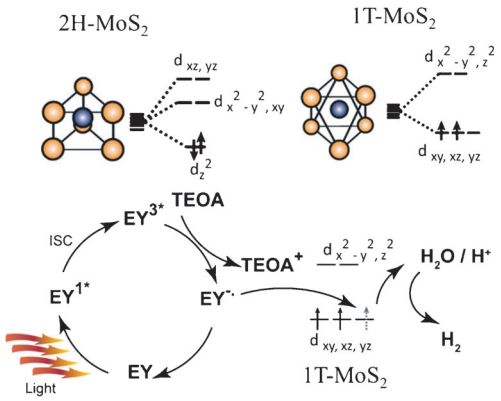

Figure 5. The crystal-field-splitting induced electronic configuration of 2H-MoS_2 and 1T-MoS_2 and proposed mechanism for catalytic activity of 1T-MoS_2. Yellow S, blue-gray Mo.

Fermi level, making it metallic. Crystal-field splitting of Mo 4d under the octahedral O_h field in the case of 1T-MoS_2 leads to three triply degenerate orbitals $4d_{xy,xz,yz}$ containing two unpaired electrons and two empty doubly degenerate orbital $4d_{x^2-y^2,z^2}$ orbitals. The incompletely filled $4d_{xy,xz,yz}$ orbital gives rise to the metallic properties of 1T-MoS_2.[21d] It is possible that easy transfer of electrons from the photogenerated species EY^- to H_2O happens through the partially filled $4d_{xy,xz,yz}$ in 1T-MoS_2 (as shown in Figure 5.). This is hindered in the case of the completely occupied $Mo4d_{z^2}$ orbital of 2H-MoS_2. Theoretical and experimental evidence in the literature support that even in the case of 2H-MoS_2, it is the metallic edge states that are catalytically active and not the 2H-type basal plane.[4b,19b,26] Further investigations to clearly understand the mechanism of catalytic H_2 evolution by 1T-MoS_2 is being carried out.

In conclusion, heavily nitrogenated graphene is effective in acting as an electron channel to few-layer 2H-MoS_2, thereby enabling high HER activity. More importantly, single-layers of the 1T polytype of MoS_2, being metallic, show extraordinary HER activity. 1T-MoS_2 is stable in water medium, but may not be as stable in the dry solid state.[31] It is possible that 1T-MoS_2 can also be stabilized by rhenium doping, with greater reliability.[21d]

Experimental Section

Synthesis: Graphite oxide (GO) was prepared by the modified Hummers method.[27] Thermally exfoliated graphene EG (3–5 layers) was obtained from GO by sudden heating to 300 °C in air. N-doped EG (NEG) was prepared by heating mixture of EG (100 mg) and urea (1 g) at 600 °C for 1 h in a N_2 atmosphere.[28] The % N in NEG, was determined to be 5 atom % by XPS. Further functionalization of NEG was needed to create a sufficient density of functional groups.[29] To prepare the graphene–MoS_2 composites, EG/NEG (20 mg) and $(NH_4)_6Mo_7O_{24}\cdot 4H_2O$ (100 mg; Merck 99 %) were dispersed in water, sonicated, and centrifuged, and the solid residue mixed with thiourea (1 g) and heated at 500 °C for 5 h in a N_2 atmosphere. To prepare reduced EG and NEG for Raman measurements graphene (3 mg) and thiourea (30 mg) were heated at 500 °C for 3 h. X-ray diffraction and HRTEM studies show that 2H-MoS_2 in the composites had 2–4 layers growing vertically on graphene with their edges exposed (TEM in Supporting Information). Reduced graphene oxide (RGO) was prepared by the reduction of SGO (single-layer graphene oxide) with $NaBH_4$.[30] RGO-MoS_2(2H) composites were prepared hydrothermally as discussed by Min and Lu.[15] EG/NEG-MoS_2 composites were similarly prepared starting from EG and NEG by hydrothermal procedures. To prepare NRGO-MoS_2, GO (30 mg), $(NH_4)_6Mo_7O_{24}\cdot 4H_2O$ (60 mg), thiourea (1.5 g) were sonicated in water (10 mL) and heated in an Teflon-lined autoclave at 220 °C for 72 h. 1T-MoS_2 was prepared by Li-intercalation of bulk MoS_2 with *n*-butyl lithium followed by exfoliation in water as reported elsewhere.[22] The sample was dried by lyophillization and annealed at 300 °C for 1 h to examine the transformation of 1T.

TEM diffraction and HRTEM were performed in a FEI TITAN cubed double aberration corrected 80–300 keV microscope. Negative C_s imaging was used ($C_s \approx -35$–40 μm, $\Delta f \approx +8$ nm) to image atoms with white contrast and direct interpretation.

Photocatalytic measurements: The catalyst (2 mg) was dispersed in water (40 mL) and triethanolamine (15 % v/v; 8 mL) as a sacrificial agent in a quartz vessel. The vessel was thoroughly purged with N_2. 0.15 mM Eosin Y was used as the sensitizer. The vessel was irradiated under 100 W halogen lamp (flux of 300 W m^{-2}) with constant stirring of the mixture. 1 mL of evolved gases were manually collected from the headspace of the vessel and analyzed in PerkinElmer Clarus ARNEL 580 gas chromatograph. For better comparison with the literature systems photocatalysis was also carried out under 400 W Xe lamp, Newport 69920 with flux of ca. 2500 W m^{-2}. Turnover frequency (TOF) for each catalyst was calculated per mole of MoS_2 present in each catalyst, considering the fact that H_2 evolution happens on MoS_2 only. Number of mole of MoS_2 in per mg of catalyst was determined from XPS and elemental analysis.

Received: August 6, 2013
Revised: September 14, 2013
Published online: November 11, 2013

Keywords: H_2 evolution · molybdenum · MoS_2 · N-doped graphene · photocatalysis

[1] a) J. Barber, *Chem. Soc. Rev.* **2009**, *38*, 185–196; b) A. Kudo, Y. Miseki, *Chem. Soc. Rev.* **2009**, *38*, 253–278.
[2] R. R. Chianelli, M. H. Siadati, M. P. De La Rosa, G. Berhault, J. P. Wilcoxon, R. Bearden, B. L. Abrams, *Catal. Rev.* **2006**, *48*, 1–41.
[3] a) A. B. Laursen, S. Kegnaes, S. Dahl, I. Chorkendorff, *Energy Environ. Sci.* **2012**, *5*, 5577–5591; b) H. Tributsch, J. C. Bennett, *J. Electroanal. Chem.* **1977**, *81*, 97–111; c) K. Sakamaki, K. Hinokuma, A. Fujishima, *J. Vac. Sci. Technol. B* **1991**, *9*, 944–949.
[4] a) B. Hinnemann, P. G. Moses, J. Bonde, K. P. Jørgensen, J. H. Nielsen, S. Horch, I. Chorkendorff, J. K. Nørskov, *J. Am. Chem. Soc.* **2005**, *127*, 5308–5309; b) T. F. Jaramillo, K. P. Jørgensen, J. Bonde, J. H. Nielsen, S. Horch, I. Chorkendorff, *Science* **2007**, *317*, 100–102.
[5] S. Helveg, J. V. Lauritsen, E. Lægsgaard, I. Stensgaard, J. K. Nørskov, B. S. Clausen, H. Topsøe, F. Besenbacher, *Phys. Rev. Lett.* **2000**, *84*, 951–954.
[6] J. Kibsgaard, J. V. Lauritsen, E. Lægsgaard, B. S. Clausen, H. Topsøe, F. Besenbacher, *J. Am. Chem. Soc.* **2006**, *128*, 13950–13958.
[7] M. Brorson, A. Carlsson, H. Topsøe, *Catal. Today* **2007**, *123*, 31–36.
[8] J. Bonde, P. G. Moses, T. F. Jaramillo, J. K. Nørskov, I. Chorkendorff, *Faraday Discuss.* **2009**, *140*, 219–231.
[9] D. Merki, S. Fierro, H. Vrubel, X. Hu, *Chem. Sci.* **2011**, *2*, 1262–1267.
[10] Y. Li, H. Wang, L. Xie, Y. Liang, G. Hong, H. Dai, *J. Am. Chem. Soc.* **2011**, *133*, 7296–7299.
[11] Z. Chen, J. Kibsgaard, T. F. Jaramillo, *Proc. SPIE* **2010**, *7770*, DOI: 10.1117/12.860659.
[12] X. Zong, Y. Na, F. Wen, G. Ma, J. Yang, D. Wang, Y. Ma, M. Wang, L. Sun, C. Li, *Chem. Commun.* **2009**, 4536–4538.
[13] Q. Xiang, J. Yu, M. Jaroniec, *J. Am. Chem. Soc.* **2012**, *134*, 6575–6578.
[14] X. Zong, H. Yan, G. Wu, G. Ma, F. Wen, L. Wang, C. Li, *J. Am. Chem. Soc.* **2008**, *130*, 7176–7177.
[15] S. Min, G. Lu, *J. Phys. Chem. C* **2012**, *116*, 25415–25424.
[16] a) F. Meng, J. Li, S. K. Cushing, M. Zhi, N. Wu, *J. Am. Chem. Soc.* **2013**, *135*, 10286–10289; b) Y. Hou, Z. Wen, S. Cui, X. Guo, J. Chen, *Adv. Mater.* **2013**, DOI: 10.1002/adma.201303116.
[17] a) R. Voggu, B. Das, C. S. Rout, C. N. R. Rao, *J. Phys. Condens. Matter* **2008**, *20*, 472204; b) A. Das, S. Pisana, B. Chakraborty, S. Piscanec, S. K. Saha, U. V. Waghmare, K. S. Novoselov, H. R. Krishnamurthy, A. K. Geim, A. C. Ferrari, A. K. Sood, *Nat. Nanotechnol.* **2008**, *3*, 210–215.
[18] H. S. S. Ramakrishna Matte, A. Gomathi, A. K. Manna, D. J. Late, R. Datta, S. K. Pati, C. N. R. Rao, *Angew. Chem.* **2010**, *122*, 4153–4156; *Angew. Chem. Int. Ed.* **2010**, *49*, 4059–4062.

[19] a) B. Hinnemann, J. K. Nørskov, H. Topsøe, *J. Phys. Chem. B* **2004**, *108*, 2245 – 2253; b) J. Kibsgaard, Z. Chen, B. N. Reinecke, T. F. Jaramillo, *Nat. Mater.* **2012**, *11*, 963 – 969.
[20] M. V. Bollinger, J. V. Lauritsen, K. W. Jacobsen, J. K. Nørskov, S. Helveg, F. Besenbacher, *Phys. Rev. Lett.* **2001**, *87*, 196803.
[21] a) V. Alexiev, R. Prins, T. Weber, *Phys. Chem. Chem. Phys.* **2000**, *2*, 1815 – 1827; b) K. E. Dungey, M. D. Curtis, J. E. Penner-Hahn, *Chem. Mater.* **1998**, *10*, 2152 – 2161; c) F. Wypych, R. Schollhorn, *J. Chem. Soc. Chem. Commun.* **1992**, 1386 – 1388; d) A. N. Enyashin, L. Yadgarov, L. Houben, I. Popov, M. Weidenbach, R. Tenne, M. Bar-Sadan, G. Seifert, *J. Phys. Chem. C* **2011**, *115*, 24586 – 24591.
[22] G. Eda, H. Yamaguchi, D. Voiry, T. Fujita, M. Chen, M. Chhowalla, *Nano Lett.* **2011**, *11*, 5111 – 5116.
[23] C. L. Jia, M. Lentzen, K. Urban, *Science* **2003**, *299*, 870 – 873.
[24] M. A. Lukowski, A. S. Daniel, F. Meng, A. Forticaux, L. Li, S. Jin, *J. Am. Chem. Soc.* **2013**, *135*, 10274 – 10277.
[25] D. Voiry, H. Yamaguchi, J. Li, R. Silva, D. C. B. Alves, T. Fujita, M. Chen, T. Asefa, V. B. Shenoy, G. Eda, M. Chhowalla, *Nat. Mater.* **2013**, *12*, 850-855.
[26] L. P. Hansen, Q. M. Ramasse, C. Kisielowski, M. Brorson, E. Johnson, H. Topsøe, S. Helveg, *Angew. Chem.* **2011**, *123*, 10335 – 10338; *Angew. Chem. Int. Ed.* **2011**, *50*, 10153 – 10156.
[27] W. S. Hummers, R. E. Offeman, *J. Am. Chem. Soc.* **1958**, *80*, 1339 – 1339.
[28] L. Xin-Jing, Y. Xin-Xin, L. Jin-Yang, F. Xiao-Dong, Z. Kun, C. Hong-Bing, P. Nan, W. Xiao-Ping, *Chin. J. Chem. Phys.* **2012**, *25*, 325.
[29] a) C. N. R. Rao, K. S. Subrahmanyam, H. S. S. R. Matte, B. Abdulhakeem, A. Govindaraj, B. Das, P. Kumar, A. Ghosh, D. J. Late, *Sci. Technol. Adv. Mater.* **2010**, *11*, 054502; b) K. S. Subrahmanyam, A. Ghosh, A. Gomathi, A. Govindaraj, C. N. R. Rao, *Nanoscale Nanotechnol. Lett.* **2009**, *1*, 28 – 31.
[30] W. Gao, L. B. Alemany, L. Ci, P. M. Ajayan, *Nat. Chem.* **2009**, *1*, 403 – 408.
[31] D. Yang, S. J. Sandoval, W. M. R. Divigalpitiya, J. C. Irwin, R. F. Frindt, *Phys. Rev. B* **1991**, *43*, 12053 – 12055.
[32] F. A. Frame, F. E. Osterloh, *J. Phys. Chem. C* **2010**, *114*, 10628 – 10633.
[33] A. Sobczynski, *J. Catal.* **1991**, *131*, 156 – 166.
[34] S. Kanda, T. Akita, M. Fujishima, H. Tada, *J. Colloid Interface Sc.* **2011**, *354*, 607 – 610.
[35] Q. Xiang, J. Yu, M. Jaroniec, *J. Am. Chem. Soc.* **2012**, *134*, 6575 – 6578.
[36] J. Djamil, S. A. Segler, A. Dabrowski, W. Bensch, A. Lotnyk, U. Schurmann, L. Kienle, S. Hansen, T. Beweries, *Dalton Trans.* **2013**, *42*, 1287 – 1292.

